The Impact of Coherent Synchrotron Radiation on the Beam Transport of Short Bunches*

R. Li
Thomas Jefferson National Accelerator Facility, 12000 Jefferson Ave., Newport News, VA 23606

Abstract

Designs for next-generation accelerators, such as future linear colliders and short-wavelength FEL drivers, require beams of short (mm-length or smaller) bunches and high charge (nC-regime). As such a high charge microbunch traverses magnetic bends, the curvature effect on the bunch self-interaction, by way of coherent synchrotron radiation (CSR) and space charge force, may cause serious emittance degradation. This impact of CSR on the beam transport of short bunches has raised significant concern in the design of future machines and led to extensive investigations. This paper reviews some of the recent progress in the understanding of the CSR effect, presents analysis of and computational work on the CSR impact on short bunch transport, and addresses remaining issues.

1 INTRODUCTION

The designs of future accelerators often require creation and manipulation of beams with high phase space densities. This incorporates short bunches with high charge being circulated or compressed by magnetic bending systems [1, 2]. The strong requirement of these designs on the preservation of small emittances makes it crucial to understand the evolution of beam phase space as a high charge microbunch traverses magnetic bends.

When an electron bunch goes through a bend, each electron gives out synchrotron radiation. When the radiation wavelength is longer than the bunch length, the radiations from individual electrons add constructively to form coherent synchrotron radiation (CSR). This coherent synchrotron radiation is a result of the curvature induced electromagnetic self-interactions within the bunch. These self-interactions may have detrimental effects on beam phase space: the longitudinal collective self-force could induce energy spread on the bunch, which further causes dispersive displacement of the particles due to the nonzero dispersion in the bend region, whereas the transverse collective self-force could directly drive the transverse motion nonuniformly across the bunch. Both the longitudinal and transverse self-interaction forces can cause emittance growth. Even when the bunch is transported through an achromatic system, since the curvature induced energy deviations occur *during* the bends, emittance degradation could still be a potential problem.

* This work is supported by the U.S. Dept. of Energy under Contract No. DE-AC05-84ER40150.

The problems related to the CSR effect in bends are: What are the curvature induced longitudinal and transverse self-interaction forces? What are their parametric dependence, their transient and steady state behavior? What is the effect of shielding by the vacuum chamber surrounding the beam? What is the impact of the curvature induced self-interaction on the short bunch transport through magnetic bending systems? What is the present understanding of the cancellation of the centrifugal space-charge force (CSCF) with the particle potential? What is the role of the non-inertial space-charge force? How does one simulate the bunch dynamics in a curved trajectory with the presence of the CSR effect? How does one handle the retardation and singularity which is intrinsic to the problem? How does one model the beam so as to maintain self-consistency of the simulation? How do the simulation results benchmark with analysis? Finally, how do the analysis and simulation compare with experiments?

This paper reviews some of the main results in the analysis, discusses the self-consistent simulation of the CSR impact on bunch dynamics, and highlights recent experiments.

2 OUTLINE OF THE CSR PROBLEM

First we outline the fundamental equations governing the curvature induced bunch self-interaction.

Consider a source electron with charge e, velocity v and acceleration $\dot{v}$. The electromagnetic field generated by the source electron at its retarded space-time $(\mathbf{r}', t')$ on a test electron at $(\mathbf{r}, t)$ is described by the Liénard-Wiechert formula: $\mathbf{E}_0 = \mathbf{E}_0^c + \mathbf{E}_0^r, \mathbf{B}_0 = \mathbf{B}_0^c + \mathbf{B}_0^r$,

$$\mathbf{E}_0^c = e\left[\frac{\mathbf{n}-\boldsymbol{\beta}}{\gamma^2(1-\boldsymbol{\beta}\cdot\mathbf{n})^3R^2}\right]_{\rm ret}, \mathbf{B}_0^c = (\mathbf{n}\times\mathbf{E}_0^c)_{\rm ret}, \quad (1)$$

$$\mathbf{E}_0^r = \frac{e}{c}\left[\frac{\mathbf{n}\times\{(\mathbf{n}-\boldsymbol{\beta})\times\dot{\boldsymbol{\beta}}\}}{(1-\boldsymbol{\beta}\cdot\mathbf{n})^3R}\right]_{\rm ret}, \mathbf{B}_0^r = (\mathbf{n}\times\mathbf{E}_0^r)_{\rm ret}, \quad (2)$$

where $\boldsymbol{\beta} = \mathbf{v}/c$, $\dot{\boldsymbol{\beta}} = \dot{\mathbf{v}}/c$, $\gamma = (1-\beta^2)^{-1}$, $\mathbf{R} = \mathbf{r}-\mathbf{r}'$, $R = |\mathbf{R}|$, and $\mathbf{n} = \mathbf{R}/R$. The subscript "ret" denotes the retardation condition

$$t' = t - |\mathbf{r}-\mathbf{r}'|/c, \quad (3)$$

which requires the fields to travel from source to test electron with the velocity of light c. Here $\mathbf{E}_0^c$ and $\mathbf{B}_0^c$ are the Coulomb fields, and $\mathbf{E}_0^r$ and $\mathbf{B}_0^r$ are the radiation fields caused by the acceleration $\dot{\boldsymbol{\beta}}$ of the source electron. The

Lorentz force applied on the test electron by the single source electron is therefore $\mathbf{F}_0(\mathbf{r},t) = \mathbf{F}_0^{\rm c} + \mathbf{F}_0^{\rm r}$, with

$$\mathbf{F}_0^{\rm c} = e(\mathbf{E}_0^{\rm c} + \boldsymbol{\beta} \times \mathbf{B}_0^{\rm c}),\ \mathbf{F}_0^{\rm r} = e(\mathbf{E}_0^{\rm r} + \boldsymbol{\beta} \times \mathbf{B}_0^{\rm r}). \quad (4)$$

Given the above single particle forces, we can now move on to discuss the collective forces generated by a bunch. For a bunch moving on a circular orbit, let s denote the initial offset of a particle from the bunch center, and the particle's trajectory as $\mathbf{r}_0(\mathbf{s},t)$. Then the bunch density distribution $n(\mathbf{r},t)$ can be expressed in terms of its initial density distribution $\lambda(\mathbf{s})$ with respect to the bunch centroid: $n(\mathbf{r},t) = \int ds\, \lambda(\mathbf{s})\delta(\mathbf{r} - \mathbf{r}_0(\mathbf{s},t))$. A test electron in the bunch will then experience the collective self-interaction forces, which are the integral of the single particle Coulomb and radiation forces in Eq. (4) generated by all the electrons in the bunch,

$$\begin{cases} \mathbf{F}^{\rm cc}(\mathbf{r},t) = \int \mathbf{F}_0^{\rm c}(\mathbf{r},t,\mathbf{s}')\lambda(\mathbf{s}')d\mathbf{s}' \\ \mathbf{F}^{\rm cr}(\mathbf{r},t) = \int \mathbf{F}_0^{\rm r}(\mathbf{r},t,\mathbf{s}')\lambda(\mathbf{s}')d\mathbf{s}' \end{cases} \quad (5)$$

where $\mathbf{F}^{\rm cc}$ stands for the *collective Coulomb force*, and $\mathbf{F}^{\rm cr}$ for the *collective radiation force*. The two collective forces have distinctive features. For steady-state circular motion, $\mathbf{F}^{\rm cc}$ is negligible at high energy while $\mathbf{F}^{\rm cr}$ is still effective. However, even at high energy, both are important for transient interaction. Therefore they should both be included when considering the feedback to the bunch dynamics

$$d(\gamma m\dot{\mathbf{v}})/dt = \mathbf{F}^{\rm ext} + \mathbf{F}^{\rm cc} + \mathbf{F}^{\rm cr}, \quad (6)$$

where $\mathbf{F}^{\rm ext}$ stands for the external force.

Instead of the integration of single particle Liénard-Wiechert fields as described above, it is often easier to analyze the bunch self-interaction forces in terms of the potentials

$$\mathbf{F} = -e\nabla(\Phi - \boldsymbol{\beta}\cdot\mathbf{A}) - ed\mathbf{A}/cdt. \quad (7)$$

However, associating the potential approach with the Liénard-Wiechert approach often can help us identify the nature of a potential term — if it is originated from the collective Coulomb force $\mathbf{F}^{\rm cc}$ or the radiation force $\mathbf{F}^{\rm cr}$.

3 ANALYSIS OF SELF-INTERACTION

In this section we study the curvature induced bunch self-interaction of a rigid Gaussian line-bunch on a circle in free space, with the particle density function

$$\lambda(s,\sigma_s) = e^{-s^2/2\sigma_s^2}/\sqrt{2\pi}\sigma_s. \quad (8)$$

Here s is the longitudinal distance from the bunch center, and σ_s is the rms bunch length. The radius of the circle is ρ and the number of electrons in the bunch is N. The velocity of the bunch is v, and $\beta = v/c$.

3.1 Steady-State Results in Free Space

The longitudinal collective force on the bunch is [3, 4, 5]

$$F_\theta(s) \simeq \frac{2Ne^2}{\sqrt{2\pi}(3\rho^2\sigma_s^4)^{\frac{1}{3}}}\int_0^\infty \frac{d\phi_1}{\phi_1^{\frac{1}{3}}}\frac{\partial}{\partial\phi_1}e^{-\frac{(s/\sigma_s-\phi_1)^2}{2}}. \quad (9)$$

This equation shows that the longitudinal force is bigger for smaller bend radius and shorter bunch length, and it causes energy spread by accelerating the bunch head and decelerating the bunch tail. For example, for $\rho = 1$ m, $\sigma_s = 1$ mm, and $N = 10^9$, we have $|F_\theta|_{\rm max} \sim 8$keV/m. The steady-state CSR power in free space (fs) is [5, 6]

$$P^{\rm fs} = -\int F_\theta(s)\lambda(s)ds \simeq \frac{N^2e^2c}{\rho^{2/3}\sigma_s^{4/3}}\frac{3^{1/6}\Gamma^2(2/3)}{2\pi}. \quad (10)$$

Using Eq. (7), the transverse collective force yields

$$F_r = -e\frac{\partial(\Phi - \boldsymbol{\beta}\cdot\mathbf{A})}{\partial r} - e\frac{dA_r}{cdt} + e\mathbf{A}\cdot\frac{d\mathbf{e}_r}{cdt}, \quad (11)$$

where the third term on the right of the equation contains the rate of change of the transverse direction, which is purely due to the curvature effect. For circular motion, this term gives the centrifugal space-charge force (CSCF) [7]:

$$F^{\rm CSCF} = e\mathbf{A}\cdot\frac{d\mathbf{e}_r}{cdt} = e\frac{\beta_\theta A_\theta}{r} \quad (12)$$

with r the distance of the test particle from the center of the design circle. It can be shown that $F^{\rm CSCF}$ is dominant in F_r of Eq. (11). For a rigid 2D Gaussian ribbon-bunch on a circular orbit with density distribution $\lambda(s,\sigma_s)\lambda(z,\sigma_z)$, with $\lambda(s,\sigma_s))$ given in Eq. (8) and z being the vertical offset from design orbit, one has [8]

$$A_\theta(s,z=0) \simeq N e\lambda(s,\sigma_s)\ln\left[\frac{(\rho\sigma_s^2)^{2/3}}{\sigma_z^2}(1+\frac{\sigma_z}{\sigma_s})\right]. \quad (13)$$

For example, for $\rho = 1$ m, $\sigma_s = 1$ mm, $\sigma_z = 1$ mm, $N = 10^9$, we have $|F^{\rm CSCF}|_{max} \sim 3$ keV/m. Similar to the coasting beam case [7], the logarithmic dependence of $F^{\rm CSCF}$ with respect to the transverse offset $x = r - \rho$ also exists for a bunched beam. This highly nonlinear behavior with transverse offset makes its impact on the transvese dynamics worrisome for machine designers. This topic will be further discussed in Sec. 4.1.

3.2 Shielding of Steady-State CSR

The mechanism of shielding of steady-state coherent synchrotron radiation by two parallel conducting plates is well understood [9, 10, 11]. Denoting the gap size between the two plates being h, and the shielding factor as

$$\eta = \sqrt{\frac{2}{3}}\left(\frac{\pi\rho}{h}\right)^{3/2}\left(\frac{\sigma_s}{\rho}\right), \quad (14)$$

we can show [12] that for strong shielding ($\eta \geq 1$), the ratio of the shielded CSR power $P^{\rm sh}$ to free-space steady-state CSR power $P^{\rm fs}$ (Eq. (10)) is given by

$$P^{\rm sh}/P^{\rm fs} \simeq 4.2\eta^{5/6}e^{-2\eta}. \quad (15)$$

The behavior of $P^{\rm sh}/P^{\rm fs}$ vs. η is depicted in Fig. 1. The free-space case corresponds to $h = \infty$, or $\eta = 0$, where $P^{\rm sh}/P^{\rm fs} = 1$. As the gap becomes narrower, η grows bigger, and the CSR is gradually shut off. For example, for $\rho = 1$ m, $\sigma_s = 1$ mm, $h = 2$ cm, we have $\eta = 1.6$, and $P^{\rm sh}/P^{\rm fs} = 0.25$.

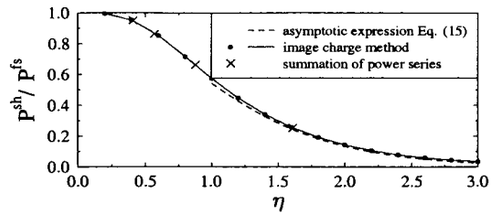

Figure 1: Steady-state CSR power with shielding, with free-space case corresponding to $\eta = 0$.

3.3 *Transient Self-Interaction with Shielding*

The free-space transient self-interaction for a bunch entering a bend from a straight path was recently studied by Saldin [13]. Later we studied the transient self-interaction in the presence of shielding [14]. To illustrate the duration and magnitude of the transients, we plot in Fig. 2 the instantaneous power $P^{sh}(t)$ (normalized by P^{fs} in Eq. (10)) radiated by a line Gaussian bunch as a function of θ, which is the angle of the bunch center entering the bend from a straight path. Here we use the typical parameters $\rho = 1$ m, $\sigma_s = 1$ mm. Fig. 2 shows that the free-space power increases from zero and saturates to its steady-state value as the bunch moves into the bend. For $h = 2$ cm, the transient power oscillates and saturates to its steady-state value after $\theta = 30°$. For machine designs intending to reduce the CSR effect by using a narrow gap size, one should notice that in a certain bend region, the transient interaction with shielding has much bigger amplitude than its steady-state counterpart, as shown by the $h = 2$ cm curve in Fig. 2 around $\theta \sim 10°$.

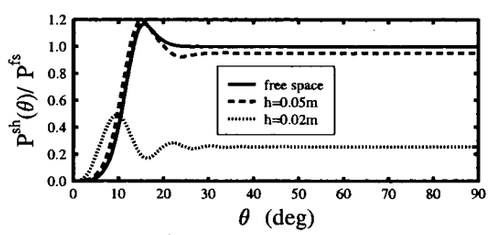

Figure 2: Transient power loss of an ultrarelativistic bunch, due to the curvature-induced self-interaction in the presence of two parallel plates, with $\rho = 1$ m, $\sigma_s = 1$ mm, and various plate spacing h. Here θ is the angle of the bunch center entering the bend.

Our study [14] also shows that the collective Coulomb force from the straight path upstream of a bend makes an important contribution to the transient self-interaction of the bunch. This is because when the bunch turns into the arc, the pancake-shaped Coulomb field from the straight path shines right upon a portion of the bunch just turned into the arc, causing the transient collective Coulomb effect comparable in magnitude with the transient collective radiation effect.

4 IMPACT ON BUNCH DYNAMICS

4.1 *General Formalism*

In the previous section, we discussed the curvature induced bunch self-interaction forces. These forces feed back on the bunch dynamics through the equation of motion in Eq. (6). Let θ be the angle of an electron into the bend, E_0 be the design energy, $x = (r-\rho)/\rho$ be the relative offset from the design orbit, and the design bending field be the only external field. Then the first order equation for the transverse motion of an electron in the bunch is [8]

$$\frac{d^2x}{d\theta^2} + x = \frac{\Delta E}{E_0} + \frac{\rho F_r}{E_0}, \tag{16}$$

where F_r is given by Eq. (11), and denoting the initial potential of the electron as Φ_0, one has

$$\Delta E = \int_0^\theta \Delta F_\theta \rho d\theta' - e(\Phi - \Phi_0),\ \Delta F_\theta = e\frac{\partial(\Phi - \boldsymbol{\beta}\cdot\mathbf{A})}{c\partial t}. \tag{17}$$

It is instructive to further write Eq. (16) as

$$\frac{d^2x}{d\theta^2} + x = \frac{e\Phi_0}{E_0} + \frac{\rho}{E_0}\left[\int_0^\theta \Delta F_\theta d\theta' + G\right]. \tag{18}$$

Here G is the residual function in which the logarithmic A_θ term (Sec.3.1) in F_r is largely cancelled with the potential Φ in Eq. (17), as shown by the underlined term:

$$\begin{aligned} G &\equiv F_r - \frac{e\Phi}{\rho} \\ &= -e\frac{\partial(\Phi - \boldsymbol{\beta}\cdot\mathbf{A})}{\partial r} - e\frac{dA_r}{cdt} + \underline{e(\frac{\beta_\theta A_\theta}{r} - \frac{\Phi}{\rho})} \\ &= G_0 + G_1 x + ... \end{aligned} \tag{19}$$

for $G_0 = G|_{x=0}$ and $G_1 = \frac{\partial G}{\partial r}\big|_{x=0}$.

The general formula in Eq. (18) applies to both the coasting beam case and the bunched beam case. For a coasting beam with constant density λ, one can show that

$$\Delta F_\theta = 0, \quad G_0 = \text{ constant}, \tag{20}$$

$$G_1 = O\left[\frac{\lambda}{\rho^2}\right] \ll \frac{\partial F_r}{\partial r}\bigg|_{x=0} \tag{21}$$

as studied by E. Lee [15]. For a bunched beam, in steady state, the driving terms in Eq. (18) are

$$\begin{aligned} &\Delta F_\theta = F_\theta \quad (F_\theta \text{ as in Eq. (9)}) \\ &G \simeq -e\frac{V_0}{\rho} - e\frac{\partial V_0}{\rho\partial x} - e\frac{\beta_\theta A_\theta}{\rho}x \end{aligned} \tag{22}$$

with $V_0 \equiv \Phi - \beta_\theta A_\theta$. Note that unlike the coasting beam, where G_0 is a constant which only modifies the equilibrium orbit, here for a bunched beam, $G_0(s)$ and $G_1(s)$ are non-uniform across the bunch, so they both could cause emittance growth. Using the result of V_0 [8], one has

$$\frac{|G_0|_{\max}}{|\Delta F_\theta|_{\max}} \sim \left(\frac{\sigma_s}{\rho}\right)^{1/3}, \quad \frac{|G_1|_{\max}x}{|\Delta F_\theta|_{\max}} \sim \frac{x}{\rho}\left(\frac{\sigma_s}{\rho}\right)^{-1/3}. \tag{23}$$

For $\sigma_s/\rho \sim 10^{-6}$ to 10^{-3}, one often has

$$x \ll (\sigma_s/\rho)^{1/3} \ll 1. \tag{24}$$

It then yields

$$\frac{|G_0|_{\max}}{|\Delta F_\theta|_{\max}} \ll 1 \quad \text{and} \quad \frac{|G_1|_{\max} x}{|\Delta F_\theta|_{\max}} \ll 1. \tag{25}$$

With the comparisons of G and ΔF_θ in Eqs. (23) and (25), one should keep in mind that in Eq. (18), the effect of the residual function G on the transverse motion should be compared with the *integral* of ΔF_θ over the bend angle $\int \Delta F_\theta d\theta'$. Therefore the comparison of the effects of G and ΔF_θ varies with different machine designs. Also note that similar to the initial energy spread, Φ_0 in Eq. (18) does not cause emittance growth for an achromatic bending system. For a line charge moving *on-axis* from a straight path to a circle, i.e., $x = 0$, the nonvanishing $(\Phi - \Phi_0)$ is purely the transient effect due to the collective Coulomb forces from the straight path [14]. Therefore the fact that Φ is largely cancelled by A_θ in Eq. (19) indicates that the on-axis A_θ undos part of the transient effects.

4.2 *Noninertial Space-Charge Force*

The role of the "noninertial space-charge force" [16] can be understood in the context of the big picture discussed in the above sections. This force arises from the analysis of the longitudinal collective force exerted on an off-axis ($x \neq 0$) test particle from a finite uniform bunch on a circle.

We start with the single particle force exerted on an observation particle O by a source particle S orbiting on a circle. Let the distances from S and O to the center of the circular orbit C be R_s and R_o respectively, $c\tau$ be the distance from S to O, and γ_s be the Lorentz factor of S. In the cylindrical coordinate, at the observation time t, O is at (R_o, θ_o) and S is at (R_s, θ_s). The corresponding retarded time for S is t' when S is at (R_s, θ_s'). The angular distances of O and S from the bunch center are $\phi_o = \theta_o - \beta_s ct/R_s$ and $\phi' = \theta_s' - \beta_s ct'/R_s$ respectively. Let $s_o = R_s\phi_o$, $s' = R_s\phi'$ and $\theta = \theta_o - \theta_s'$. For $\Delta s = s_o - s'$, the retardation relation requires

$$R_s\theta = \Delta s + \beta_s c\tau, \quad c\tau = \sqrt{R_s^2 + R_o^2 - 2R_sR_o\cos\theta}. \tag{26}$$

The *single particle* longitudinal force from S on O is

$$F_{\theta 0} = -e\frac{\partial\Phi}{R_o\partial\theta} - e\frac{\partial A_\theta}{c\partial t} =$$

$$-e^2\frac{\partial}{\partial\Delta s}\left[\frac{\frac{R_s}{\gamma_s^2 R_o} + \beta_s^2\left(\frac{R_s}{R_o} - 1\right) + \beta_s^2(1-\cos\theta)}{c\tau - \beta_s R_o\sin\theta}\right] \tag{27}$$

where θ and τ are implicit functions of Δs via Eq. (26).

The *collective* longitudinal force on the test particle O is

$$F_\theta(s_o) = \int_{s_r}^{s_f} F_{\theta 0}(s_o - s')\lambda(s')ds'$$

$$\simeq e^2\lambda\left[\frac{\frac{R_s}{\gamma_s^2 R_o} + \beta_s^2\left(\frac{Rs}{R_o} - 1\right) + \beta_s^2(1-\cos\theta)}{c\tau - \beta_s R_o\sin\theta}\right]_{s_o - s_r}^{s_o - s_f} \tag{28}$$

with λ the constant bunch density, and s_r and s_f standing for the rear and front of the line bunch respectively. Comparing the *single particle* force in Eq. (27) with the Liénard-Wiechert fields in Eqs. (1) and (2), one finds that on the right-hand side of Eq. (27)), the first term is the Coulomb field and the second and third terms are the radiation field. Therefore in the *collective* force of Eq. (28), the first term is the collective Coulomb force and the second and third terms are the collective radiation force.

The longitudinal collective force can also be analyzed using the potential approach. For $\beta_o = \beta_s$ one has

$$F_\theta(s_o) = e\left[\frac{\partial(\Phi - \boldsymbol{\beta}_o\cdot\mathbf{A})}{c\partial t} - \frac{d\Phi}{cdt}\right] \tag{29}$$

$$\simeq e^2\lambda\left[\frac{\frac{1}{\gamma_s^2} + \left(\frac{R_s}{R_o} - 1\right) + \beta_s^2(1-\cos\theta)}{c\tau - \beta_s R_o\sin\theta}\right]_{s_o - s_r}^{s_o - s_f} \tag{30}$$

Notice that Eq. (30) is equivalent to Eq. (28) but slightly varied in expression. In the literature [16], for the terms on the right-hand side of Eq. (30), the first term is called the "usual Coulomb force", the second term is named the "noninertial space-charge force" and the third term is called the " usual CSR force". One can show that the "noninertial space-charge" term is nothing but the $-ed\Phi/cdt$ term in Eq. (29), which integrated over time gives the term $-e(\Phi - \Phi_0)$ in Eq. (17) for the energy change. As we've shown in Eq. (19), the effect of the potentials Φ in the energy change is largely cancelled by the term A_θ in F_τ, and only the residual of their cancellation, the function G, acts as one of the driving factors to the transverse motion. Therefore we remark that the effect of the "noninertial space-charge force" on the transverse motion must be considered *together* with the radial force (Talman's force) so as to have a complete and proper description of the dynamical system.

5 SELF-CONSISTENT SIMULATION

The analyses in the previous sections are based on the rigid-line-bunch model. In reality, a bunch has finite transverse size, and its dynamics responds to the curvature induced self-interaction. In order to study the actual dynamical system, we have developed a *self-consistent* simulation [17] based on a 2-dimensional macroparticle model. This simulation integrates numerically the following equation of motion around a design orbit

$$\frac{d(\gamma\beta_r)}{cdt} - \beta_\theta\left(\frac{\gamma\beta_\theta}{r} - \frac{\gamma_0\beta_0}{r_0}\right) = \tilde{F}_r \tag{31}$$

$$\frac{d(\gamma\beta_\theta)}{cdt} + \beta_r\left(\frac{\gamma\beta_\theta}{r} - \frac{\gamma_0\beta_0}{r_0}\right) = \tilde{F}_\theta, \tag{32}$$

where β_0, γ_0 are the design parameters, r_0 the design radius, $B_{\text{ext}} = -e\gamma_0\beta_0\mathbf{e}_z/r_e r_0$ for $r_e = e^2/mc^2$, and $\tilde{\mathbf{F}} = (e/mc^2)(\mathbf{E} + \boldsymbol{\beta}\times\mathbf{B})$ is the curvature induced self-interaction force in free space. The algorithm for the computation of the curvature induced self-interaction force $\tilde{\mathbf{F}}$

and its benchmark with analytical results are described in Ref.[17], which shows that the macroparticle model handles the retardation and self-consistency in a straightforward manner.

In Ref.[17] it is shown that the fields from each macroparticle are 2-dimensional integrals over the area surrounding the previous path of the source macroparticle. The singularities in the integrands are intrinsic to the Green's function and are readily removed by integration by parts using the finite 2-dimensional size of the macroparticles. By doing this, one finds that as the result of the retardation relation, the integrand of F_r has a narrow spike near the observation point (in addition to the long range behavior), which has nontrivial contribution to the integration. Therefore extra care is needed for the numerical integration to compute F_r.

The above described simulation can handle both transient (including entrance and exit) and steady-state self-interaction self-consistently. It also takes care of cases involving the coupling of two or more bends, where the radiation generated in an earlier bend can influence the bunch when it is at succeeding bends. The disadvantage of the above scheme is that it takes extra numerical work to calculate the radial force correctly, while this force is actually largely canceled with Φ, which is hidden in γ of Eq. (31) as part of ΔE. Therefore this scheme *indirectly* handles the cancellation of F_r and Φ.

To overcome the disadvantage in the above scheme, we are currently improving the simulation by numerically integrating the following reduced form of the equation of motion:

$$\begin{cases} \dfrac{d(\gamma+\tilde{\Phi})\beta_r}{cdt} - \beta_\theta\left[\dfrac{(\gamma+\tilde{\Phi})\beta_\theta}{r} - \dfrac{\gamma_0\beta_0}{\rho}\right] \\ \qquad = -\dfrac{\partial\tilde{V}_0}{\partial r} + \beta_\theta\dfrac{\delta\tilde{A}_\theta}{r} - \dfrac{d\delta\tilde{A}_r}{cdt} \\ \dfrac{d(\gamma+\tilde{\Phi})\beta_\theta}{cdt} + \beta_r\left[\dfrac{(\gamma+\tilde{\Phi})\beta_\theta}{r} - \dfrac{\gamma_0\beta_0}{\rho}\right] \\ \qquad = -\dfrac{\partial\tilde{V}_0}{\rho\partial\theta} - \beta_\theta\dfrac{\delta\tilde{A}_r}{r} - \dfrac{d\delta\tilde{A}_\theta}{cdt} \\ \dfrac{d(\gamma+\tilde{\Phi})}{dt} = \dfrac{\partial\tilde{V}_0}{\partial t} \end{cases} \tag{33}$$

where the reduced potentials are

$$\tilde{\Phi} = \frac{e}{mc^2}\Phi \qquad \tilde{V}_0 = \frac{e}{mc^2}(\Phi - \boldsymbol{\beta}\cdot\mathbf{A})$$
$$\delta\tilde{A}_{r,\theta} = \frac{e}{mc^2}(A_{r,\theta} - \beta_{r,\theta}\Phi). \tag{34}$$

In this new scheme, $\delta\tilde{A}_\theta$ is the residual of the cancellation of Φ and A_θ, whose effect on the transverse dynamics can be clearly identified. With the initial potential $\Phi(t=0)$ known, one can obtain at each step $(\beta_r, \beta_\theta, \gamma+\tilde{\Phi})$ as the result of the driving factors $\nabla\tilde{V}_0$ and $\delta\tilde{\mathbf{A}}$. These driving factors are computed from the macroparticle model as 2-dimensional integrals in a similar way as the field calculation in Ref.[17]. Notice that due to the above mentioned cancellation, when computing the driving factors in Eq. (6), the retardation-caused local spikes in the integrands have now negligible contribution to the integrals; therefore they are numerically much easier to compute than the radial force F_r in the previous scheme. Our numerical computation shows that for a line charge, the numerical results of the driving factors agree with their analytical counterparts. These numerical results are not sensitive to the macroparticle size as long as it is much less than the real bunch size. Development of simulation based on this new scheme is still continuing.

6 RECENT EXPERIMENTS

Recently there are some experimental results on the CSR effect in bends. One example is the measurement of the transverse emittances as a function of bending angle carried out on the CLIC bunch compressor [18], which shows that among all the possible causes of transverse phase space dilation, the CSR effect can best explain the measured emittance growth. On the Jefferson Lab FEL beamline, we are in the process of measuring the emittance growth through the first 180° arc as a function of the cryomodule phase. The latter rotates the longitudinal phase space and affects the bunch length along the beamline in a complex way. Currently we are carrying out parametric studies of the CSR effect using the simulation, and systematic benchmarking of the simulation with experiment is underway at Jefferson Lab.

The author thanks C. Bohn, J. J. Bisognano and P. Emma for many helpful discussions. The support of NERSC for the parallel computing on the T3E machine is also gratefully acknowledged.

7 REFERENCES

[1] M. Cornacchia, SLAC-PUB-7433, 1997.
[2] E. T. d'Amico, et al., CLIC Note 355, 1998.
[3] L. V. Iogansen and M. S. Rabinovich, Sov. Phys. JETP **37**(10), 83 (1960).
[4] Ya. S. Derbenev, et al., DESY Report No. TESLA-FEL-95-05, 1995.
[5] B. Murphy, S. Krinsky, and R. L. Gluckstern, BNL-63090, (1996).
[6] L. I. Schiff, Rev. Sci. Instr.17, 6-14, (1946).
[7] R. Talman, *Phys. Rev. Letts.* **56**, 1429 (1986).
[8] Ya. S. Derbenev and V. Shiltsev, Fermilab-TM-1974 (1996).
[9] J. S. Nodvick and D. S. Saxon, Phys. Rev. **96**, 180 (1954).
[10] R. L. Warnock and P. Morton, Part. Accel. **25**, 113 (1990).
[11] S. Heifets and A. Michailichenko, SLAC Note AP-83 (1990).
[12] R. Li, C. L. Bohn, and J. J. Bisognano, Proceedings of the Particle Accelerator Conference, Vancouver, 1997.
[13] E. L. Saldin, E. A. Schneidmiller, and M. V. Yurkov, DESY-TESLA-FEL-96-14, (1996).
[14] R. Li, C. L. Bohn, and J. J. Bisognano, Proc. SPIE, San Diego (1997).
[15] E. P. Lee, *Particle Accelerators*, **25**, p.241 (1990).
[16] B. E. Carlsten, *Phys. Rev. E*, **54**, p.838 (1996).
[17] R. Li, Proc. of 1998 European Partical Accelerator Conf., Stockholm (1998); *Nucl. Instr. and Meth. in Phys. Res. A*, to be published.
[18] H. Braun, et al., CLIC Note 389, 1999.